was more reactive than the α-hydrogen on the bromide. Methylene produced by photolysis of ketene or diazomethane reacts with CH_3Cl, CH_2Cl_2, or CH_2Br_2 by hydrogen or halogen abstraction, but not to an appreciable extent by insertion.[29] Setser et al.[30] has reported that singlet CH_2 abstracts only chlorine and triplet CH_2 abstracts only hydrogen from CH_2Cl, although the rate constants are of comparable magnitude. Therefore, relative rates and relative reactivity cross sections will depend on excess energy and the electronic state of the carbene.

With CH_3Cl no distinction[29] can be made between Cl and H abstraction reactions of CH_2. The reaction of CH_2 and CH_3F is quite slow relative to CH_3Cl, but methylene has a greater reaction rate[31] with CH_3Br relative to CH_3Cl. In the reactions of methylene in 1/1/10 mixtures of CH_3Cl, CH_3Br, and CF_4 or in the absence of CF_4, a relative reaction rate of 1.3 favored CH_2 reactions[32] with CH_3Br relative to CH_3Cl. If the substrate is CH_3Cl, CH_2Cl_2, or CH_2Br, the CH_2 may abstract halogen, but for CH_2F_2 only halogen abstraction occurs. This is not unexpected since neither carbenes produced by photolytic means[33] or atomic carbon produced by recoil reactions[5,6c] does not insert appreciably into C–F bonds. Methylene abstracted the halogen from CH_3Cl or CH_3Br, but F abstraction was not found in CH_3F systems.[33] Intuitively, one would expect similarities between photolytically produced carbenes and those produced by nuclear transformations.

Acknowledgment. This research was carried out at Brookhaven National Laboratory under contract with the U.S. Department of Energy and supported by its Division of Basic Energy Sciences and its Office of Health and Environmental Research. Discussions with E. P. Rack are acknowledged with appreciation.

Registry No. CH_4, 74-82-8; CH_3F, 593-53-3; CH_2F, 75-10-5; CHF_3, 75-46-7; CF_4, 75-73-0; CH_3Cl, 74-87-3; CH_2Cl_2, 75-09-2; $CHCl_3$, 67-66-3; CCl_4, 56-23-5; CH_3Br, 74-83-9; CH_2Br_2, 74-95-3; $CHBr_3$, 75-25-2; CH_3I, 74-88-4; C_2H_6, 74-84-0; C_2H_5Cl, 75-00-3; CH_3CHCl_2, 75-34-3; CH_3CF_2Cl, 75-68-3; CH_3CCl_3, 71-55-6; $ClCF_3$, 75-72-9; ICF_3, 2314-97-8; $HClCF_2$, 75-45-6; Cl_2CF_2, 75-71-8; HCl_2CF, 75-43-4; Cl_3CBr, 75-62-7; C_2F_2, 689-99-6; C_4F_{10}, 355-25-9; c-C_4F_8, 115-25-3; C_6F_{14}, 355-42-0; C_6H_6, 71-43-2; C_6F_6, 392-56-3; C_6F_5H, 363-72-4; 1,2,3,4-$C_6F_4H_2$, 551-62-2; 1,2,4,5-$C_6F_4H_2$, 327-54-8; $C_6F_5CF_3$, 434-64-0; c-$C_6F_{11}CF_3$, 355-02-2; ^{11}C, 14333-33-6.

Supplementary Material Available: Additional experimental details and Figures S1–S4 showing the radiolytic studies of the $CF_4 + O_2$, c-$C_4F_8 + O_2$, and $CH_4 + O_2$ systems (9 pages). Ordering information is given on any current masthead page.

(29) (a) C.H. Bamford, I. E. Casson, and R. P. Wayne, *Proc. R. Soc. London, Ser. A*, **289**, 287 (1965); (b) J. C. Hassler, D. W. Setser, and R. J. Johnson, *J. Chem. Phys.*, **45**, 3231 (1966).
(30) W. G. Clark, D. W. Setser, and E. E. Siefert, *J. Phys. Chem.*, **74**, 1670 (1970).
(31) G. O. Pritchard, J. T. Bryant, and R. L. Thommerson, *J. Phys. Chem.*, **69**, 2804 (1965).
(32) R. L. Johnson and D. W. Setser, *J. Phys. Chem.*, **71**, 4366 (1967).
(33) F. Casan, J. A. Kerr, and A. F. Trotman-Dickerson, *J. Chem. Soc.* **201**, 1141 (1965).

Kinetics and Mechanism of HO_2 and DO_2 Disproportionations

Carl C. Kircher† and Stanley P. Sander*

Jet Propulsion Laboratory, California Institute of Technology, Pasadena, California 91109
(Received: June 20, 1983)

The $HO_2 + HO_2$ and $DO_2 + DO_2$ reactions in the gas phase have been studied by the flash photolysis/UV absorption technique. Rate constants were measured at pressures between 100 and 700 torr of Ar and N_2 at temperatures between 230 and 420 K, and with up to 10 torr of added water vapor The overall disproportionation rate constant can be expressed as the sum of pressure-independent and pressure-dependent terms. For the $HO_2 + HO_2$ reaction, $k_1 = 2.3 \times 10^{-13} \exp(600/T) + 8.4 \times 10^{-34}[M] \exp(1100/T)$ cm^3 molecule^{-1} s^{-1} for M = Ar and $k_1 = 2.2 \times 10^{-13} \exp(620/T) + 1.9 \times 10^{-33}[M] \exp(980/T)$ cm^3 molecule^{-1} s^{-1} for M = N_2. For the $DO_2 + DO_2$ reaction, $k_2 = 2.2 \times 10^{-14} \exp(900/T) + 3.6 \times 10^{-34}[M] \exp(1200/T)$ cm^3 molecule^{-1} s^{-1} for M = N_2. The experimental uncertainty in k_1 and k_2, including systematic errors, is 25% (one standard deviation). The enhancement of the $HO_2 + HO_2$ rate constant in the presence of added water vapor was studied over the temperature range 250–298 K and found to contribute a multiplicative term $(1 + 1.4 \times 10^{-21} \exp(2200/T)[H_2O])$ to the rate constant expressions. The mechanism of the $HO_2 + HO_2$ reaction was investigated with a two-channel RRKM model which suggested that the binding energy of the HO_4H intermediate lies in the range of 12–20 kcal mol^{-1} relative to HO_2 reactants.

Introduction

The bimolecular disproportionation of HO_2 radicals

$$HO_2 + HO_2 \rightarrow H_2O_2 + O_2 \quad (1)$$

shows a number of interesting features. In particular, the pressure dependence of the reaction has come under intense scrutiny with a number of conflicting results being reported.[1-4] A recent study from our laboratory[1] at 298 K showed that both bimolecular and termolecular pathways were operative in reaction 1 and that the observed rate constant could be expressed as the sum of pressure-dependent and pressure-independent terms

$$k_1 = k_{II} + k_{III}[M] \quad (I)$$

This was in apparent conflict with at least one low-pressure study which found no bimolecular component and a much larger value for k_{III}.[4] In addition, if our pressure dependence is correct, then the overall temperature dependence of k_1 would be expected to depend on the pressure. While several recent temperature-dependence studies have been performed,[2,5-7] only one has noted a pressure-dependent activation energy.

† NASA/NRC Resident Research Associate.

(1) S. P. Sander, M. Peterson, R. T. Watson, and R. Patrick, *J. Phys. Chem.*, **86**, 1236 (1982).
(2) R. A. Cox and J. P. Burrows, *J. Phys. Chem.*, **83**, 2560 (1979).
(3) R-R. Lii, R. A. Gorse, Jr., M. C. Sauer, Jr., and S. Gordon, *J. Phys. Chem.*, **84**, 813 (1980).
(4) B. A. Thrush and J. P. T. Wilkinson, *Chem. Phys. Lett.*, **66**, 441 (1979).
(5) R-R. Lii, R. A. Gorse, Jr., M. C. Sauer, Jr., and S. Gordon, *J. Phys. Chem.*, **83**, 1803 (1979).
(6) R. Patrick and M. J. Pilling, *Chem. Phys. Lett.*, **91**, 343 (1982).
(7) B. A. Thrush and G. S. Tyndall, *Chem. Phys. Lett.*, **92**, 232 (1982).

0022-3654/84/2088-2082$01.50/0

TABLE I: Rate Constants for $HO_2 + HO_2 \rightarrow H_2O_2 + O_2$

T, K	$10^{12}k$,[a] cm^3 molecule^{-1} s^{-1}				
			Ar Carrier Gas		
240	3.31 ± 0.28 (79.3)	3.51 ± 0.10 (150)	3.71 ± 0.24 (250)	4.28 ± 0.15 (400)	4.55 ± 0.26 (555.6)
268	2.16 ± 0.13 (90.4)	2.47 ± 0.15 (300)	2.84 ± 0.10 (500)	3.16 ± 0.28 (626.9)	3.26 ± 0.17 (700)
298[b]	1.80 ± 0.27 (100)	1.91 ± 0.29 (200)	2.10 ± 0.32 (350)	2.17 ± 0.33 (500)	2.52 ± 0.38 (700)
333	1.36 ± 0.08 (111.5)	1.50 ± 0.12 (300)	1.59 ± 0.10 (400)	1.75 ± 0.04 (600)	1.85 ± 0.18 (781.3)
417	1.02 ± 0.10 (139.6)	1.17 ± 0.08 (300)	1.17 ± 0.13 (500)	1.28 ± 0.08 (700)	1.21 ± 0.10 (992.5)
			N_2 Carrier Gas		
241	3.50 ± 0.17 (100)	4.00 ± 0.20 (200)	4.54 ± 0.31 (350)	4.89 ± 0.10 (500)	6.07 ± 0.16 (600)
269	2.41 ± 0.11 (100)	2.68 ± 0.13 (200)	2.89 ± 0.10 (350)	3.38 ± 0.18 (500)	3.55 ± 0.24 (700)
298[b]	1.91 ± 0.29 (100)	2.10 ± 0.32 (200)	2.36 ± 0.35 (350)	2.61 ± 0.39 (500)	2.97 ± 0.45 (700)
344	1.35 ± 0.05 (100)	1.52 ± 0.05 (200)	1.62 ± 0.14 (350)	1.75 ± 0.10 (500)	2.15 ± 0.13 (700)
417	1.08 ± 0.13 (100)	1.11 ± 0.08 (200)	1.20 ± 0.12 (350)	1.27 ± 0.08 (500)	1.30 ± 0.17 (700)

[a] Total pressure in parentheses (torr). Uncertainties are one standard deviation. [b] Reference 1.

The need for accurate measurements of k_1 stems from the importance of the reaction in atmospheric and combustion chemistry, and its use as a reference reaction in other kinetics studies. In this work we have investigated the effects of pressure and temperature on both the bimolecular and termolecular components of k_1. We also examined the enhancement of the reaction rate by the addition of water vapor, a phenomenon observed in several previous studies.[1,2,8-10] In order to further elucidate the reaction mechanism, we studied the temperature and pressure dependence of the analogous reaction involving DO_2

$$DO_2 + DO_2 \rightarrow D_2O_2 + O_2 \quad (2)$$

The above measurements were used to construct a two-channel RRKM model which was used to investigate the energetics and structural properties of the reaction intermediates.

Experimental Section

The HO_2 radicals in this study were generated by flash photolysis within a Pyrex flash lamp/reaction cell and were monitored spectrophotometrically at 227.5 nm. The apparatus has been described in detail previously.[11,12] Briefly, the spectrophotometer system employed a deuterium lamp source, an 0.5-m monochromator with a 2.0-nm spectral bandpass, and an EMI 9781A photomultiplier tube. Kinetic decays obtained from about 100 flashes were signal averaged by a multichannel analyzer to obtain a detection limit of about 0.1% absorption. The flash energy was varied between 500 and 1000 J/flash. The absorption path length from eight passes of the analytical beam was 670 ± 14 cm. The temperature of the photolysis cell was held constant by circulating ethylene glycol or 2-propanol through the cell's temperature control jacket. A heat exchanger containing 2-propanol and dry ice was included in the temperature control system for kinetic measurements below 260 K.

The following reaction scheme was used to generate HO_2 and DO_2:

$$Cl_2 + h\nu\ (\lambda > 300\ \text{nm}) \rightarrow 2Cl \quad (3)$$

$$Cl + CH_3OH\ (CD_3OD) \rightarrow HCl\ (DCl) + CH_2OH\ (CD_2OD) \quad (4)$$

$$CH_2OH\ (CD_2OD) + O_2 \rightarrow HO_2\ (DO_2) + HCHO\ (DCDO) \quad (5)$$

The reactant concentrations were (in molecules cm^{-3}) $[Cl_2] = (1.5\text{–}15) \times 10^{15}$, $[CH_3OH\ (CD_3OD)] = (1.0\text{–}5.0) \times 10^{15}$, and $[O_2] = (1.5\text{–}4.0) \times 10^{17}$. Ar and N_2 were used as the diluent gases. The gas concentrations employed and the reaction rates of (4) and (5) were such that the HO_2 (DO_2) radicals were generated within 15 μs, much shorter than the millisecond time scale of the HO_2 disproportionation.

The absorption cross sections at 227.5 nm used in the calculations of the second-order rate constant were (in cm^2 molecule^{-1}) $(3.0 \pm 0.4) \times 10^{-18}$ for HO_2,[1] $(2.5 \pm 0.33) \times 10^{-18}$ for DO_2,[1] and 2.14×10^{-19} for H_2O_2.[13] Although these values were measured at room temperature, the cross sections were not expected to vary significantly with temperature since the HO_2 and DO_2 absorption bands are continua and the analyzing wavelength lies near the peak of the absorption. Since spectral data were not available for D_2O_2, the cross section at 227.5 nm was estimated from the relation

$$\sigma_{D_2O_2} = \sigma_{H_2O_2}(\sigma_{DO_2}/\sigma_{HO_2})$$

yielding a value of 1.8×10^{-19} cm^2 molecule^{-1}. Fortunately, the derived rate constant is fairly insensitive to the D_2O_2 cross section with a worst-case error of 4% being expected if the cross section were zero.

Because HO_2 disproportionation follows second-order kinetics, plots of reciprocal optical density (base e) vs. time are linear with slopes equal to $2k_1/\sigma$ (or $2k_2/\sigma$ for DO_2) where σ is the effective HO_2 cross section given by

$$\sigma = \sigma_{HO_2} - \sigma_{H_2O_2}/2$$

with a similar relationship existing for DO_2. The correction arises from the residual absorption from H_2O_2. In this paper, rate constants are defined by the equation

$$-d[HO_2]/dt = 2k_1[HO_2]^2$$

In order to perform experiments with water vapor present, a bubbler was immersed in a thermostated water bath and connected to the carrier gas stream. Saturation of the carrier gas stream with water vapor has been demonstrated previously.[1] The water vapor pressure within the photolysis cell was controlled by the water bath temperature (0–20 °C), the tank regulator pressure (5–25 psi), the position of the bubbler relative to the carrier gas needle valve (upstream or downstream), and the flow rate through a bypass carrier gas stream.

Results

For each of five temperatures in the range 230–420 K, rate constants for hydroperoxyl radical disproportionation were measured between 100 and 700 torr by using both N_2 and Ar diluents, an expansion of our earlier study which utilized several different third bodies but was limited to $T = 298$ K. Plots of the second-order rate constant vs. N_2 pressure are shown in Figure 1 with the data for Ar carrier gas having the same general appearance. These rate constants are tabulated in Table I. Each point represents the average of the rate constants for 8–10 kinetics runs in which $[HO_2]_0$, $[Cl_2]$, $[CH_3OH]$, and $[O_2]$ were varied over factors of 3–5. The 298 K data were published in our earlier study.[1] The measured rate constants at all temperatures were

(8) E. J. Hamilton and R-R. Lii, *Int. J. Chem. Kinet.*, **9**, 875 (1977).
(9) W. B. DeMore, *J. Phys. Chem.*, **83**, 1113 (1979).
(10) R-R. Lii, M. C. Sauer, Jr., and S. Gordon, *J. Phys. Chem.*, **85**, 2833 (1981).
(11) R. T. Watson, S. P. Sander, and Y. L. Yung, *J. Phys. Chem.*, **83**, 2936 (1979).
(12) S. P. Sander and R. T. Watson, *Chem. Phys. Lett.*, **77**, 473 (1981).
(13) L. T. Molina, S. D. Schinke, and M. J. Molina, *Geophys. Res. Lett.*, **4**, 580 (1977).

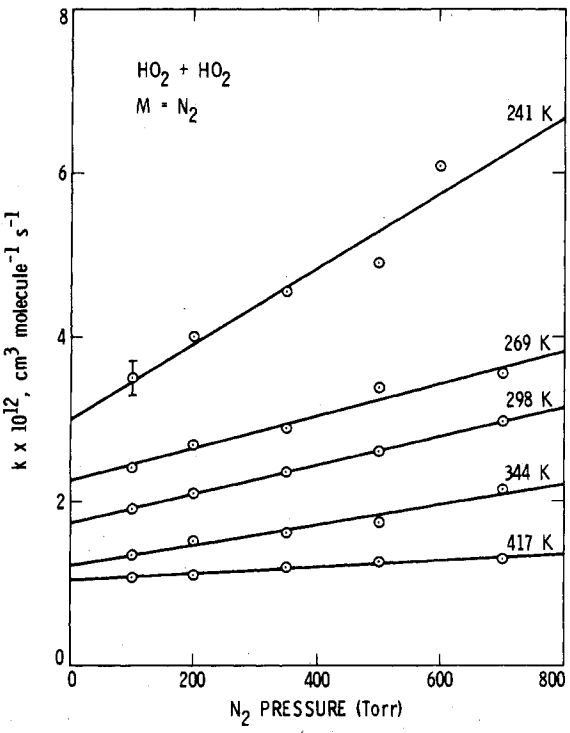

Figure 1. Variation of the $HO_2 + HO_2$ rate constant with N_2 pressure and temperature. Error bars are one standard deviation.

TABLE II: Bimolecular and Termolecular Rate Constants for HO_2 Disproportionation

T, K	$10^{12}k_{II}$,[a] cm^3 molecule^{-1} s^{-1}	$10^{32}k_{III}$,[a] cm^6 molecule^{-2} s^{-1}
	Ar Carrier Gas	
417	1.06 ± 0.10	0.92 ± 0.35
333	1.28 ± 0.10	2.6 ± 0.8
298	1.68 ± 0.18	3.5 ± 2.0
268	1.96 ± 0.16	5.1 ± 1.2
240	3.14 ± 0.20	6.2 ± 1.5
	N_2 Carrier Gas	
417	1.05 ± 0.18	1.7 ± 1.1
344	1.22 ± 0.10	4.4 ± 1.0
298	1.74 ± 0.22	5.4 ± 3.1
269	2.26 ± 0.15	6.5 ± 0.7
241	3.00 ± 0.18	11.4 ± 0.9

[a] Errors are one standard deviation.

observed to vary linearly with pressure, supporting our earlier suggestion[1] that the reaction consists of a bimolecular channel and a termolecular channel in the low-pressure limiting region. Linear regressions of the data at each temperature gave the y intercepts and slopes listed in Table II. These values represent the bimolecular (k_{II}) and termolecular (k_{III}) rate constants, respectively, in eq I. Arrhenius plots of k_{II} and k_{III} for both carrier gases (shown in Figures 2 and 3) were linear within experimental error. The Arrhenius expressions are

Ar:

$$k_{II} = 2.3 \times 10^{-13} \exp((600 \pm 130)/T) \text{ cm}^3 \text{ molecule}^{-1} \text{ s}^{-1}$$

$$k_{III} = 8.4 \times 10^{-34} \exp((1100 \pm 300)/T) \text{ cm}^6 \text{ molecule}^{-2} \text{ s}^{-1}$$

N_2: $$k_{II} = 2.2 \times 10^{-13} \exp((620 \pm 60)/T) \text{ cm}^3 \text{ molecule}^{-1} \text{ s}^{-1}$$

$$k_{III} = 1.9 \times 10^{-33} \exp((980 \pm 200)/T) \text{ cm}^6 \text{ molecule}^{-2} \text{ s}^{-1}$$

The estimated experimental uncertainty in k_1 and k_2, including systematic errors, is 25% (one standard deviation). Rate constants for reaction 1 were also measured over the temperature range 230–420 K with the diluent gas density held constant at Ar number densities of 3.23×10^{18} and 2.27×10^{19} molecules cm^{-3} which correspond to 100 and 700 torr at 298 K, respectively. The rate

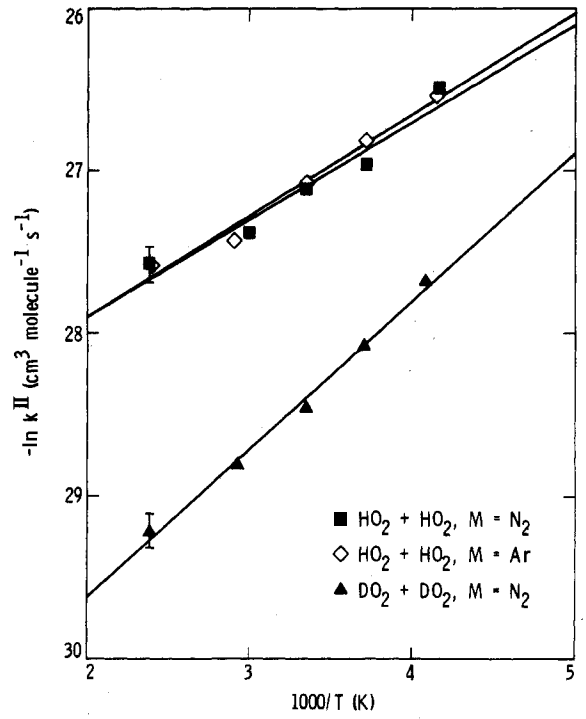

Figure 2. Temperature dependence of the bimolecular HO_2 and DO_2 disproportionation rate constants.

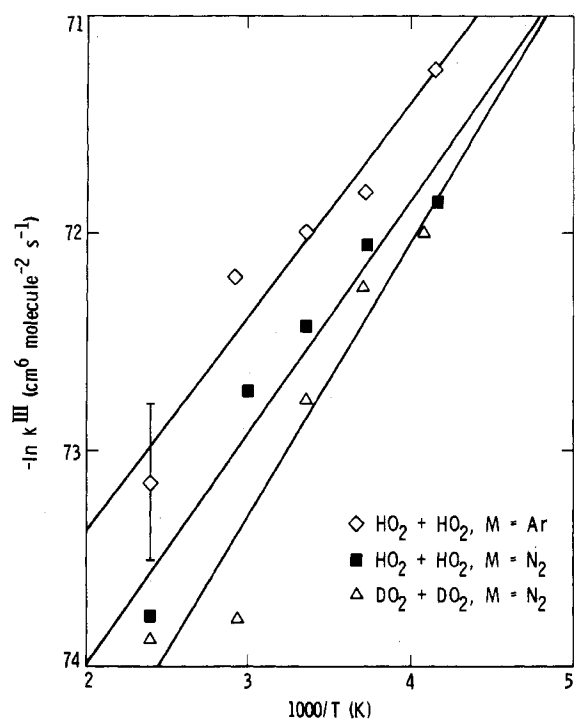

Figure 3. Temperature dependence of the termolecular HO_2 and DO_2 disproportionation rate constants.

constants obtained from these experiments are plotted in Figure 4. The following Arrhenius expressions were obtained:

$$[M] = 3.23 \times 10^{18} \text{ molecules cm}^{-3}$$

$$k = 2.3 \times 10^{-13} \exp((610 \pm 100)/T) \text{ cm}^3 \text{ molecule}^{-1} \text{ s}^{-1}$$

$$[M] = 2.27 \times 10^{19} \text{ molecules cm}^{-3}$$

$$k = 2.2 \times 10^{-13} \exp((720 \pm 100)/T) \text{ cm}^3 \text{ molecule}^{-1} \text{ s}^{-1}$$

For comparison, rate constants for the same conditions of pressure, temperature, and third body were calculated with eq I and the

TABLE III: Rate Constants for $DO_2 + DO_2 \rightarrow D_2O_2 + O_2$, $M = N_2$

	$10^{12}k$,[a] cm^3 $molecule^{-1}$ s^{-1}				
T, K	100 torr	200 torr	350 torr	500 torr	700 torr
245	1.18 ± 0.06	1.38 ± 0.05	1.69 ± 0.09	1.81 ± 0.09	2.27 ± 0.07[c]
270	0.80 ± 0.04	0.92 ± 0.09	1.16 ± 0.04	1.40 ± 0.09	1.68 ± 0.09
298[b]	0.53 ± 0.05	0.60 ± 0.03	0.72 ± 0.05	0.82 ± 0.08	1.03 ± 0.08
342	0.33 ± 0.02	0.38 ± 0.02	0.40 ± 0.02	0.44 ± 0.02	0.49 ± 0.05
418		0.25 ± 0.01	0.27 ± 0.02	0.30 ± 0.01	0.32 ± 0.03[c]

[a] Errors are one standard deviation. [b] Data at 200, 350, and 500 torr from ref 1. [c] Data at 245 and 418 K measured at 600 torr.

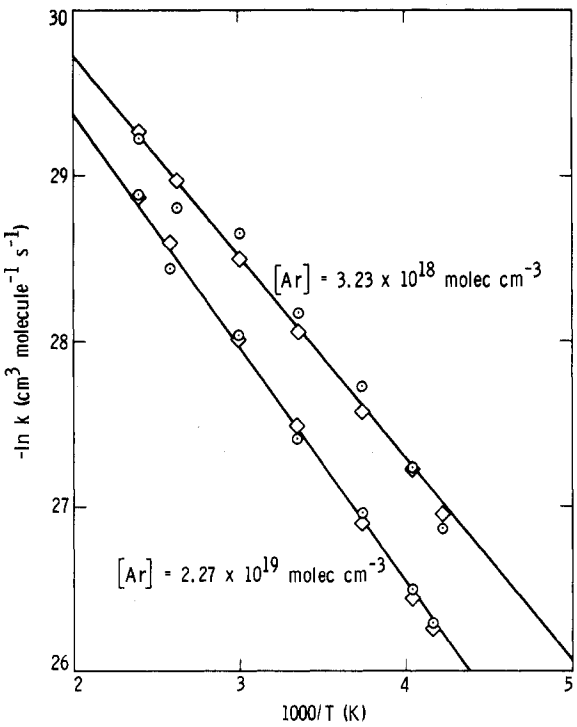

Figure 4. Temperature dependence of $HO_2 + HO_2$ rate constants at constant Ar number density: (⊙) observed rate constant; (—) least-squares line through experimental points; (◇) rate constants calculated from $k_{II} + k_{III}[Ar]$.

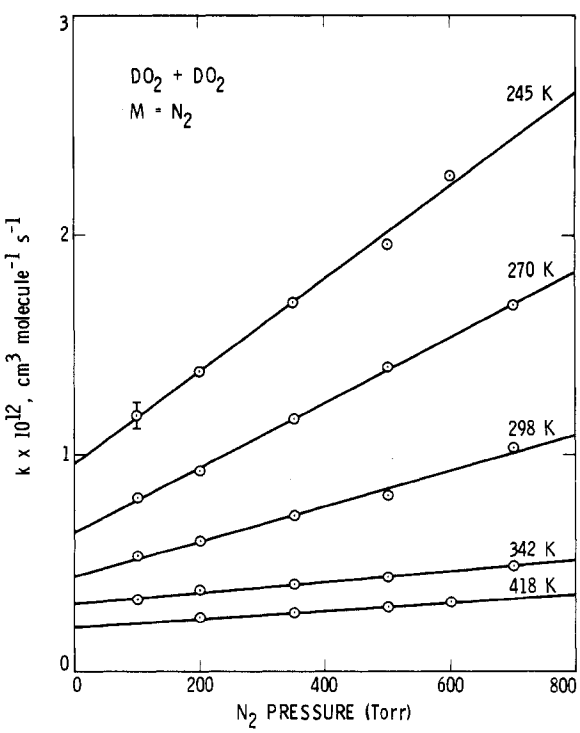

Figure 5. Variation of the $DO_2 + DO_2$ rate constant with N_2 pressure and temperature. Error bars are one standard deviation.

TABLE IV: Bimolecular and Termolecular Rate Constants for DO_2 Disproportionation

T, K	$10^{13}k_{II}$,[a] cm^3 $molecule^{-1}$ s^{-1}	$10^{32}k_{III}$,[a] cm^6 $molecule^{-2}$ s^{-1}
418	2.05 ± 0.29	0.83 ± 0.38
342	3.11 ± 0.25	0.91 ± 0.33
298	4.39 ± 0.59	2.5 ± 0.7
270	6.40 ± 0.59	4.2 ± 0.6
245	9.56 ± 0.89	5.4 ± 0.7

[a] Errors are one standard deviation.

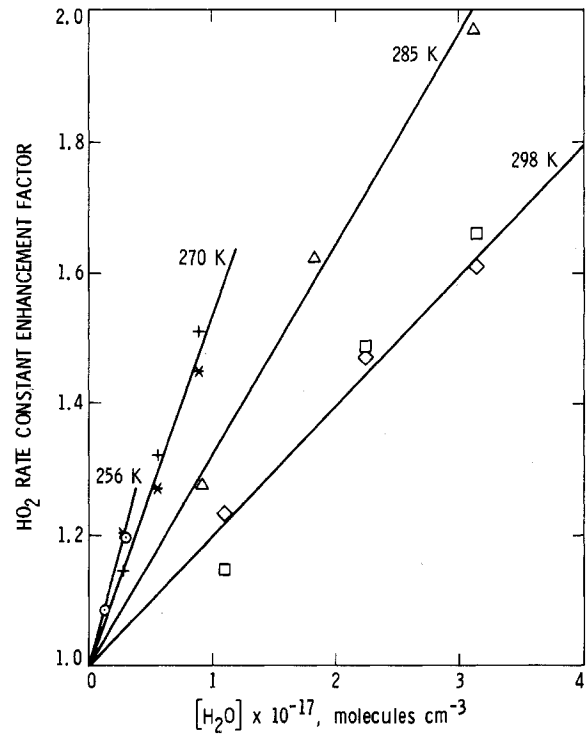

Figure 6. Enhancement (k_1/k_1^0) of the $HO_2 + HO_2$ rate constant in the presence of added water vapor, $M = N_2$: (□) p = 100 torr, 298 K; (◇) p = 700 torr, 298 K; (△) p = 100 torr, 285 K; (+) p = 100 torr, 270 K; (*) p = 700 torr, 270 K; (⊙) p = 100 torr, 256 K.

experimental values of $k_{II}(T)$ and $k_{III}(T)$. As shown in Figure 4 the agreement between the two sets of values is excellent, showing that eq I may be interpolated over a wide range of conditions.

Results from the experiments on DO_2 disproportionation were treated in a manner similar to the HO_2 experiments. Rate constants for reaction 2 are tabulated in Table III. These values were generally smaller than those for reaction 1 but showed the same qualitative dependence on pressure and temperature, as shown in Figure 5 and Table IV. Figures 2 and 3 show the temperature dependences of the bimolecular and termolecular rate constants. For DO_2, experiments were performed with only N_2 as the diluent gas. The Arrhenius expressions for k_{II} and k_{III} were determined to be

$$k_{II} = 2.2 \times 10^{-4} \exp((900 \pm 90)/T)\ cm^3\ molecule^{-1}\ s^{-1}$$

$$k_{III} = 3.6 \times 10^{-34} \exp((1200 \pm 200)/T)\ cm^6\ molecule^{-2}\ s^{-1}$$

TABLE V: Water Vapor Dependence of k_1

T, K	$p_{tot}^{N_2}$, torr	$10^{-17}[H_2O]$, molecule cm^{-3}	$10^{12}k_1$, cm^3 molecule^{-1} s^{-1}	$10^{30}k_7K$,[b] cm^6 molecule^{-2} s^{-1}
298[a]	100	0.0	1.91	3.8 ± 0.4
	100	1.10	2.19	
	100	2.24	2.84	
	100	3.14	3.17	
	100	4.41	3.59	
	700	0.0	2.97	5.8 ± 0.6
	700	1.10	3.66	
	700	2.24	4.37	
	700	3.14	4.78	
	700	4.41	5.54	
285	100	0.0	2.31	7.3 ± 0.7
	100	0.918	2.95	
	100	1.83	3.75	
	100	3.12	4.55	
270	100	0.0	2.41	14 ± 1.4
	100	0.279	2.76	
	100	0.561	3.18	
	100	0.883	3.64	
	700	0.0	3.55	17 ± 1.7
	700	0.279	4.27	
	700	0.561	4.51	
	700	0.888	5.14	
256	100	0.0	2.71	18 ± 1.8
	100	0.125	2.94	
	100	0.295	3.24	

[a] Data from ref 1. [b] Obtained from the expression $k_1 = k_1^0 + k_7K[H_2O]$ (see text).

The dependence of the $HO_2 + HO_2$ rate constant on the pressure of added water vapor was measured at 285, 270, and 256 K at 100 torr total pressure of N_2. The results are listed in Table V and plotted in Figure 6 as a water vapor enhancement factor, $k_1([H_2O])/k_1([H_2O] = 0)$. The data for 298 K were reported earlier.[1] As observed by Lii et al.[10] and Cox and Burrows,[2] the rate constant enhancement increases rapidly with decreasing temperature; at 256 K the enhancement is 3.7 times higher than at 298 K.

Decay profiles of HO_2 were observed to be second-order under all conditions of temperature and added water vapor. Cox and Burrows observed departures from second-order kinetics at low temperatures in their water vapor experiments, which were attributed to surface reactions involving adsorbed water vapor. Because our experiments were carried out on time scales much shorter than the wall diffusion time, these complications did not occur.

At 270 K, the water vapor effect was studied at total pressures of 100 and 700 torr of N_2. As in our previous experiments at 298 K, no pressure dependence of the water vapor effect was observed.

Discussion

Comparison with Previous Studies. Four previous studies of the temperature dependence of k_1 have been reported.[2,5-7] As indicated in Table VI, these studies encompass a wide range of pressure (7–1200 torr) and diluent gases (H_2, N_2, SF_6). Since, as we have shown, the reaction has both bimolecular and termolecular components, the observed temperature dependence is expected to vary at least slightly with total pressure and diluent gas. Comparisons between studies carried out in different pressure regimes must therefore be made with caution.

The previously measured temperature dependences (E/R) fall into two groups: high values around −1200 K (ref 2 and 5) and low values around −600 K (ref 6 and 7). There is no particular correlation between these measurements and the pressure regime of the experiment although Cox and Burrows[7] observed a shift in E/R from −581 to −1250 K as the pressure was increased from 10 to 760 torr. The effective temperature dependence for M = Ar as observed in this study is not a strong function of pressure, varying from −603 K in the low-pressure limit to −721 K at atmospheric pressure. Our results are therefore most consistent with the lower group of measurements. The results of Thrush and Tyndall[7] near the low-pressure limit, $k_1 = 2.4 \times 10^{-13} \exp((560 \pm 200)/T)$ cm^3 molecule^{-1} s^{-1}, compare particularly well with our expression for the bimolecular component, $k_1^{II} = (2.3 \pm 0.6) \times 10^{-13} \exp((603 \pm 132)/T)$ cm^3 molecule^{-1} s^{-1}, derived from the M = Ar data.

Arrhenius Parameters. The Arrhenius parameters for the bimolecular component of the $HO_2 + HO_2$ reaction should be independent of the diluent gas since they refer to the zero-pressure limit of the reaction. This is consistent with the observations. The measured bimolecular A factor for argon, $(2.3 \pm 0.6) \times 10^{-13}$ cm^3 molecule^{-1} s^{-1}, is nearly identical with that measured for nitrogen, $(2.2 \pm 0.5) \times 10^{-13}$ cm^3 molecule^{-1} s^{-1}. Similarly the bimolecular E/R values compare very well: (600 ± 130) K for M = Ar and (620 ± 60) K for N_2. The termolecular A factors are expected to differ by a factor corresponding to the relative collision efficiencies of the diluent gases. In this study the termolecular A-factor ratio (N_2:Ar) is 2.3 ± 0.7. This is somewhat higher than the average of the ratios of the corresponding termolecular rate constants for $HO_2 + HO_2$ at the five temperatures of this study, which was (1.64 ± 0.24). The latter value is probably the most reliable since the determination of the A factors involve a long extrapolation. This ratio is also more consistent with the relative collision efficiencies for other association reactions involving similar molecules. The temperature dependences of the termolecular components, E/R = (980 ± 200) K for N_2 and (1100 ± 300) K for Ar, agree within experimental error, which is consistent with the weak dependence of the third-body efficiency on temperature.

Water Vapor Effect. Lii et al.[10] accounted for their observations of the water vapor dependence of k_1 with a multistep mechanism that assumes that a rapid equilibrium exists in the formation of water-complexed HO_2. In their scheme, complexed HO_2 reacts with both complexed and uncomplexed HO_2.

$$HO_2 + HO_2 \rightarrow H_2O_2 + O_2 \quad (1)$$

$$HO_2 + H_2O \rightleftharpoons HO_2{\cdot}H_2O \quad (6, -6)$$

$$HO_2 + HO_2{\cdot}H_2O \rightarrow HO_2 + O_2 + H_2O \quad (7)$$

TABLE VI: Comparison of Previous Temperature-Dependence Studies on $HO_2 + HO_2$

investigators	technique[a]	diluent gas(es)	press. range, torr	temp range, K	rate constant expression[b]
Cox and Burrows[2]	MM/UV	N_2	760	273–339	$(3.8 \pm 1.4) \times 10^{-14} \exp((1250 \pm 200)/T)$
	MM/UV	N_2	10	273–339	$(2.6 \pm 0.4) \times 10^{-13} \exp((581 \pm 44)/T)$
Lii et al.[5]	PR/UV	H_2	1200	276–400	$(1.14 \pm 0.16) \times 10^{-13} \exp((1050 \pm 45)/T)$
Patrick and Pilling[6]	FP/UV	N_2	700	298–510	$(4.14 \pm 1.15) \times 10^{-13} \exp((630 \pm 115)/T)$
Thrush and Tyndall[7]	FP/IR	N_2, SF_6	7–20	298–358	$2.4 \times 10^{-13} \exp((560 \pm 200)/T)$
this work	FP/UV	Ar	80–992	240–417	$2.3 \times 10^{-13} \exp((600 \pm 130)/T) + 8.4 \times 10^{-34}[Ar] \exp((1100 \pm 300)/T)$
this work	FP/UV	N_2	100–700	241–417	$2.2 \times 10^{-13} \exp((620 \pm 60)/T) + 1.9 \times 10^{-33}[N_2] \exp((980 \pm 200)/T)$
this work ($DO_2 + DO_2$)	FP/UV	N_2	100–700	245–418	$2.2 \times 10^{-14} \exp((900 \pm 90)/T) + 3.6 \times 10^{-34}[N_2] \exp((1200 \pm 20)/T)$

[a] PR, pulse radiolysis; MM, molecular modulation; FP, flash photolysis; UV, ultraviolet absorption; IR, infrared absorption. [b] Units of bimolecular rate constants: cm^3 molecule^{-1} s^{-1}. Units of termolecular rate constants: cm^6 molecule^{-2} s^{-1}.

$$HO_2{\cdot}H_2O + HO_2{\cdot}H_2O \rightarrow H_2O_2 + O_2 + 2H_2O \quad (8)$$

If complexed and uncomplexed HO_2 have identical absorption cross sections, then the observed rate constant is given by

$$k_1 = \frac{k_1^0 + k_7K[H_2O] + k_8K^2[H_2O]^2}{(1 + K[H_2O])^2} \quad \text{(II)}$$

where $K = k_6/k_{-6}$ and k_1^0 refers to the condition where $[H_2O] = 0$. Lii et al. obtained estimates for k_7, k_8, and K by fitting their data on the water vapor dependence of k_1 to eq II. This procedure can be simplified by noting that Lii et al.,[10] Cox and Burrows,[2] and ourselves all observe a linear dependence of k_1 on $[H_2O]$. This will be the case if $K[H_2O] << 1$ and $k_8K[H_2O] << k_7$. Equation II then reduces to

$$k_1 = k_1^0 + k_7K[H_2O]$$

Values of k_7K, obtained by least-squares fitting to this equation, are listed in Table V.

The main shortcoming of this mechanism is that it fails to account for the effect of diluent gas density on the rate constant enhancement. As indicated by the data at 298 and 270 K in Table V, k_7K is pressure dependent, increasing significantly between 100 and 700 torr at both temperatures. This is consistent with the observation (Figure 6) that the rate constant enhancement factor (k_1/k_1^0) is independent of pressure. The plots in Figure 6 are best described by the equation

$$k_1 = k_1^0(1 + A_w[H_2O] \exp(-E_w/R_T))$$

It can then be shown that

$$k_7K = A_w(k_{II} + k_{III}[M]) \exp(-E_w/RT)$$

which points out the explicit dependence of k_7K on pressure and temperature. The best fits to the data in Table V are obtained with $A_w = 1.4 \times 10^{-21}$ and $E_w/R = -2200$ K. The complete expression for the observed rate constant for $M = N_2$ is then

$$k_1(T,[N_2],[H_2O]) = (2.2 \times 10^{-13} \exp(620/T) + 1.9 \times 10^{-33}[N_2] \exp(980/T))(1 + 1.4 \times 10^{-21} \exp(2200/T)[H_2O])$$

The pressure dependence of k_7K probably arises from k_7 alone since the equilibrium constant for the formation of the complex should be pressure independent. Since reaction 1 is pressure

$$HO_2 + HO_2 \rightarrow H_2O_2 + O_2 \quad (1)$$

dependent, the analogous reaction involving H_2O, written as the overall process

$$HO_2 + HO_2{\cdot}H_2O \rightarrow H_2O_2 + O_2 + H_2O \quad (7)$$

should be pressure dependent as well. The origin of the pressure dependence in both reactions will be discussed in the next section.

Several explanations have been proposed for the water vapor enhancement of the HO_2 disproportionation. The most plausible is that originally proposed by Cox and Burrows[2] who point out that the larger number of available vibrational modes in the complexed H_2O_4 species will result in a longer lifetime with respect to dissociation to reactants than for the uncomplexed form. This explanation also accounts for our observation[14] of a substantial waer vapor enhancement in the reaction, $HO_2 + NO_2 + M \rightarrow HO_2NO_2 + M$. In this reaction, like the $HO_2 + HO_2$ reaction, the enhancement is much too large to be accounted for by the increased vibrational quenching efficiency of H_2O relative to N_2.

RRKM Modeling. Since the behavior of the $HO_2 + HO_2$ reaction in the zero-pressure and low-pressure limits is fairly well quantified, some insight into the detailed mechanism can be obtained by matching RRKM calculations[15] to experimental observations. Prior to the most recent studies, Tsang[16] carried out such calculations using a two-channel model and found that no combination of reasonable transition-state structures and bond energies could reproduce the body of data then existing, i.e., the extremely high third-order rate constant measured by Thrush and Wilkinson,[4] and the low high-pressure limiting rate constant implied by the data of Cox and Burrows.[2] In view of the considerably different experimental picture presented here and in our previous study,[11] another look at this problem is required.

There are still some questions as to the yield of H_2O_2 product in reaction 1 and the possibility of an H_2 product channel.[2,11,17,18] For the simplest case of H_2O_2 as the only product, at least two distinguishable H_2O_2 transition states must be involved in the reaction mechanism, one leading to H_2O_2 (disproportionation) and the other back to reactants (dissociation). The reaction scheme may be written

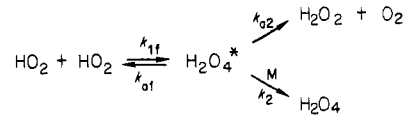

The energy barrier E_1 and E_2 corresponding to the two unimolecular reaction channels are defined relative to the H_2O_4 zero-point energy. If the steady-state assumption is used on $H_2O_4^*$, the apparent rate constant for HO_2 disappearance (defined in the usual fashion for second-order reactions) becomes

$$k_{obsd} = \frac{k_{1f}(k_{a2} + k_2[M])}{k_{a1} + k_{a2} + k_2[M]} \quad \text{(III)}$$

Equation III has the correct qualitative pressure dependence, having a finite bimolecular intercept

$$k_{II} = \frac{k_{1f}k_{a2}}{k_{a1} + k_{a2}}$$

and a termolecular component having a linear pressure dependence in the low-pressure limiting region $(k_2[M] << k_{a1} + k_{a2})$

$$k_{III} = \frac{k_{1f}k_2[M]}{k_{a1} + k_{a2}}$$

The high-pressure limit must be independent of the unimolecular and quenching processes and is therefore equal to the association rate constant

$$k_\infty = k_{1f}$$

The RRKM equation for the two-channel model is derived in an analogous fashion to the single-channel case.[15] The rate constants k_{a1} and k_{a2} are functions of the nonfixed vibrational and rotational energy of $H_2O_4^*$, E^*. Equation III may be rewritten

$$dk_{obsd} = \frac{K_1(E^*)(k_{a2}(E^*) + k_2[M])}{1 + \frac{k_{a2}(E^*)}{k_{a1}(E^*)} + \frac{k_2[M]}{k_{a1}(E^*)}} f(E^*)\, dE^* \quad \text{(IV)}$$

where $K_1(E^*)$ is the equilibrium constant for reactions 1f and a1 in the energy range E^* to $E^* + dE^*$ and $f(E^*)$ is the thermal Boltzmann distribution function given by

$$f(E^*) = \frac{k_{a1}(E^*)N^*(E^*) \exp(-E^*/kT)}{\int_{E_0}^{\infty} k_{a1}(E^*)N^*(E^*) \exp(-E^*/kT)\, dE^*}$$

$K_1(E^*)$ can be expressed as a ratio of translational, vibrational,

(14) S. P. Sander and M. E. Peterson, submitted to J. *Phys. Chem.*
(15) P. J. Robinson and K. A. Holbrook, "Unimolecular Reactions", Wiley, London, 1972.
(16) W. Tsang, Report FAA-EE-80-45, Federal Aviation Administration, Washington, DC, 1980.
(17) H. Niki, P. D. Maker, C. M. Savage, and L. P. Breitenbach, *Chem. Phys. Lett.*, 73, 43 (1980).
(18) K. A. Sahetchian, A. Heiss, R. Rigny, and R. I. Ben-aim, paper presented at the 7th International Symposium on Gas Kinetics, Gottingen, West Germany, 1982.

rotational, and electronic partition functions[15,19]

$$K_1(E^*) = (Q_{H_2O_4}/Q_{HO_2}{}^2)_{\text{trans,vib, rot, elec}}$$

$$K_1(E^*) = \left(\frac{\pi kTm}{h^2}\right)^{-3/2}\left(\frac{\omega_{H_2O_4}e^{E_1/kT}}{\omega_{HO_2}{}^2}\right) \times \left(\frac{T^{-3/2}\theta_A\theta_B\theta_C}{\pi^{1/2}(\theta_A'\theta_B'\theta_C')^{1/2}}\right)\left(\frac{N^*(E^*)e^{-E^*/kT}}{\left(\prod_{i=1}^{3}\left(1-\frac{h\nu_i}{kT}\right)^{-1}\right)^2}\right) = KN^*(E^*)e^{-E^*/kT}$$

where m is the HO_2 molecular mass, ω is the electronic spin multiplicity, θ_i is the rotational temperature $= h^2/(8\pi^2Ik)$, and $N^*(E^*)$ is the density of quantum states for $H_2O_4{}^*$ at energy E^*. In this expression primed quantities refer to H_2O_4 and unprimed quantities refer to HO_2.

The observed rate constant is obtained by integrating eq IV over E^* from E_1 to ∞. After making the change of variables

$$E^* = E^+ + E_1$$

$$dE^* = dE^+$$

where E^+ is the nonfixed energy of the activated complexes, the exponential energy term in the electronic partition function cancels. We then have

$$k_{obsd} = K\int_0^\infty \frac{(k_{a2}(E^*) + \lambda ZpF)N^*(E^*)e^{-E^+/kT}}{1 + \frac{k_{a2}(E^*)}{k_{a1}(E^*)} + \frac{\lambda ZpF}{k_{a1}(E^*)}} f(E^*)\, dE^+$$

For the first-order quenching rate $k_2[M]$ we have substituted the expression λZpF where λ is the collision efficiency between $H_2O_4{}^*$ and the diluent gas, Z is the bimolecular collision frequency, p is the total pressure, and F is the Waage–Rabinovitch factor accounting for angular momentum conservation among the adiabatic rotations.[15] This formulation assumes that all collisions between $H_2O_4{}^*$ and the diluent gas will result in vibrational quenching and that effects due to energization will be negligible. This will be the case for potential wells more than a few kilocalories deep. For shallower wells, an additional factor multiplying the λZpF term should be employed; however, given the many other uncertainties which are involved in the collision expression, energization effects can be neglected.

The specific rate constant for the ith reaction channel is given by

$$k_{ai}(E^*) = \frac{1}{hN^*(E^*)}\sum P_i(E_{vr}{}^+)$$

where $\sum P_i(E_{vr}{}^+)$ is the sum of the vibrational states of transition state i below energy E^+. $N^*(E^*)$ was calculated with the Whitten–Rabinovitch approximation while $\sum P_i(E_{vr}{}^+)$ was obtained from a direct count of states.[20]

Several possibilities have recently been suggested for the geometries of H_2O_4 and the relevant transition states. From the isotope exchange studies of Niki et al.,[17] the intermediate structure

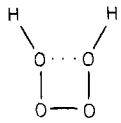

can be ruled out. One possible structure involves the initial formation of a doubly hydrogen bonded HO_2 dimer in the form of a six-membered ring followed by ring cleavage to form H_2O_2 and O_2, i.e.

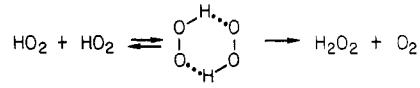

Giguere argues in favor of this mechanism on the grounds that, with an expected dimerization energy of 15 kcal mol^{-1}, the cyclic structure would be more strongly bound than covalent (open-chain) H_2O_4.[21] Diem et al. also interpret their observations of HO_2 formation in an O_2 matrix between 12 and 20 K as leading to the formation of the cyclic dimer.[22] Several ab initio calculations have recently been carried out, however, which suggest that the noncyclic zigzag H_2O_4 is also bound.[23–25] Nangia and Benson[25] estimate the binding energy for zigzag H_2O_4 relative to HO_2 fragments to be 8.9 kcal mol^{-1}, although the estimate is reduced to 5.9 kcal mol^{-1} if Shum and Benson's recent recommendation[26] of 3.5 kcal mol^{-1} is used for the HO_2 heat of formation. For H_2O_3, the same thermochemical method[25] yields −15.7 kcal mol^{-1} for $\Delta H_f°(298)$ but a recent ab initio calculation which accurately predicts the H_2O_2 heat of formation gives −26.5 kcal mol^{-1} for H_2O_3.[27] Noncyclic H_2O_4 may therefore be considerably more stable than predicted by the thermochemical methods. If the initial association of two HO_2 radicals leads to the zigzag structure, then the disproportionation must proceed via a four-center transition state

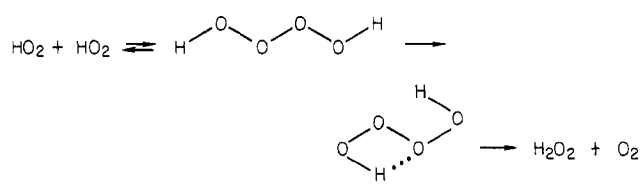

While this implies a tight complex for the product reaction channel, the energetics are favorable; Plesnicar et al. estimate the energy difference between the zigzag and four-member ring structures to be only 6 kcal mol^{-1}.[23]

The transition-state parameters used in these calculations are derived from the Gorin or restricted rotor model described by Benson,[28] and used by Golden and co-workers[29,30] in several RRKM calculations of simple fission reactions. In this model, the relative motions of the two fission fragments in the activated complex are treated as hindered internal rotations. The degree of hindrance is treated as a parameter having a value between zero and one which multiplies the moments of inertia of the internal rotors and is adjusted to give the correct temperature dependence for the high-pressure limit. This treatment is based on the idea that the position of the centrifugal barrier maximum, and thus the interfragment distance, is temperature dependent. Without this correction, RRKM theory usually fails to predict the correct temperature dependence of k in both magnitude and sign for addition reactions involving loose complexes such as OH + NO_2 + M. This problem has been discussed in detail by several authors.[29–33] Our model uses two parameters to adjust the internal moments of inertia of the complexes. α_1 is a hindrance parameter which multiplies the assumed unhindered moment of inertia of the 2-D rotor of the dissociation complex. I_1 is an absolute moment

(19) D. A. McQuarrie, "Statistical Mechanics", Harper and Row, New York, 1976.
(20) W. L. Hase and D. L. Bunker, RRKM Program available from the Quantum Chemistry Program Exchange.

(21) P. A. Giguere, *J. Phys. Chem.*, **85**, 3733 (1981).
(22) M. Diem, T-L. Tso, and E. K. C. Lee, *J. Chem. Phys.*, **76**, 6452 (1982).
(23) B. Plesnicar, S. Kaiser, and A. Azman, *J. Am. Chem. Soc.*, **95**, 5476 (1973).
(24) T. Minato, S. Yanabe, H. Fujimoto, and K. Fukui, *Bull. Chem. Soc. Jpn.*, **51**, 682 (1978).
(25) P. S. Nangia and S. W. Benson, *J. Phys Chem.*, **83**, 1138 (1979).
(26) L. G. S. Shum and S. W. Benson, *J. Phys. Chem.*, **87**, 3479 (1983).
(27) D. Cremer, *J. Comp. Chem.*, in press.
(28) S. W. Benson, "Thermochemical Kinetics", 2nd ed, Wiley, New York, 1976.
(29) G. P. Smith and D. M. Golden, *Int. J. Chem. Kinet.*, **10**, 489 (1978).
(30) A. C. Baldwin and D. M. Golden, *J. Phys. Chem.*, **82**, 644 (1978).
(31) J. Troe, *J. Phys. Chem.*, **83**, 114 (1979).
(32) I. W. M. Smith, "Kinetics and Dynamics of Elementary Gas Reactions", Butterworths, London, 1980.
(33) M. Quack and J. Troe, *Ber. Bunsenges. Phys. Chem.*, **81**, 329 (1977).

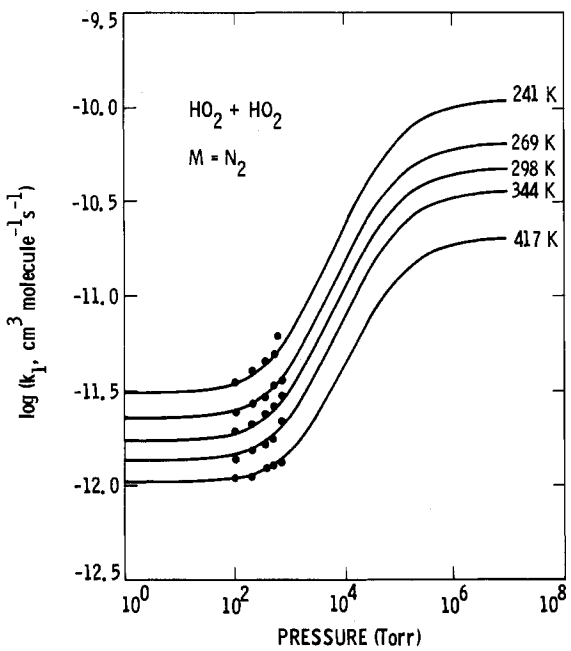

Figure 7. Falloff curves for $HO_2 + HO_2$, $M = N_2$ from RRKM calculations. Experimental points from this study are indicated. The calculations used energy barriers of 20.0 and 12.0 kcal mol^{-1} for the dissociation and disproportionation channels, respectively. Other parameters are indicated in the text.

of inertia of the internal 1-D rotor of the disproportionation complex. The other unknown parameters in the model are k_∞(298 K), the two energy barriers E_1 and E_2, and the collision efficiency λ at 298 K. The latter parameter was given a value of 0.4 at 298 K for $M = N_2$ and recalculated at other temperatures from the relation[31]

$$\frac{\lambda}{1-\lambda^{1/2}} = \frac{\langle \Delta E \rangle}{1.1kT}$$

where $\langle \Delta E \rangle$, the average energy transferred per collision, is assumed to be independent of temperature.

Because neither the energy barriers nor the hindrance parameters are well known a priori, there is considerable arbitrariness in the specification of the model. As a first guess for vibrational frequencies and internal and external moments of inertia, we have used the model developed by Tsang.[16] The hindrance parameter α_1 was then chosen to give the entropy change required to obtain an assumed value of k_∞ at 298 K. In view of the large value observed for the $OH + HO_2$ rate constant at 1 atm, $k \sim 1 \times 10^{-10}$ cm^3 molecule^{-1} s^{-1},[34] a value of 5×10^{-11} cm^3 molecule^{-1} s^{-1} was chosen for k_∞. The sensitivity of the model to this parameter is discussed below. Values of E_1 and E_2 were then chosen to match both the zero-pressure intercept k_{II}(298 K) and the observed falloff curve at 298 K. The values of E_1 and E_2 required to fit the data, 32.0 and 11.6 kcal mol^{-1} are unrealistically large. In particular, this value of E_1 is larger than the O–O bond energy in O_3 which is only 25.4 kcal mol^{-1}. Furthermore, the calculated value of E_2 would place the lifetime of stabilized H_2O_4 in the 10–100-μs regime, which is not consistent with experimental observations.[1,6,7]

Equally apparent is that to match the estimated H_2O_4 binding energy of 6–9 kcal mol^{-1} estimated by Benson[25,26] would require an extremely loose model for H_2O_4. We therefore adopted a compromise set of frequencies by lowering the frequencies of the O–O stretches, O–O–O bends, and internal torsions to the values indicated in Table VII (model II). This resulted in values of 20.0 and 8.0 kcal mol^{-1} for E_1 and E_2, respectively. With these barriers and frequencies, the parameters α_1 and I_1 were chosen to fit the data over the temperature range 241–417 K.

The resulting falloff curves are shown in Figure 7. For a given set of frequencies, the sensitivity of the model to changes in the assumed value of the high-pressure limit was examined. Reducing k_∞ to 2×10^{-11} cm^3 molecule^{-1} s^{-1}, the probable lower limit for this parameter, required a change of about 2 kcal mol^{-1} in E_1 and 1 kcal mol^{-1} in E_2. The model is also reasonably insensitive to changes in the estimate for λ.

Several interesting observations can be made on the basis of the predicted falloff curves. The true high-pressure limit is clearly not reached except at very high pressures. At 298 K, $p_{1/2}$ is about 100 atm of N_2, which points out the need for experiments in this regime to verify the calculations. In the 100–1000-torr range, only a small amount of falloff is predicted. At 1000 torr and 298 K, the calculated rate constant is about 5% less than that obtained by extrapolating from the low-pressure limit. Finally, the predicted temperature dependence of the high-pressure limit has a $T^{-2.5}$ dependence which is substantially greater than one normally

(34) W. B. DeMore, *J. Phys. Chem.*, **86**, 121 (1982).

TABLE VII: RRKM Calculations–Structural Parameters and Results[a]

H_2O_4*

mode	vibration, cm^{-1} model I	vibration, cm^{-1} model II
ν_1 OH sym stretch, ν_8 OH asym stretch	3600	3600
ν_2 OH sym bend, ν_9 OH asym bend	1300	1300
ν_3 OO sym stretch, ν_4 OO med stretch, ν_{10} OO asym stretch	800	500
ν_5 OOO sym bend, ν_{11} OOO asym bend	500	300
ν_6 torsion, ν_{12} torsion	450	300
ν_7 torsion	150	75
	rotational moments of inertia, g cm^2	
external (inactive)	6×10^{-39} (1-D) 13×10^{-39} (2-D)	

$H_2O_4^{\ddagger}$ (Dissociation Complex)

mode	vibrations (from HO_2), cm^{-1}
ν_1 OH stretch	3400 (2)
ν_2 bend	1360 (2)
ν_3 OO stretch	1120 (2)
	rotational moments of inertia, g cm^2
external (inactive)	6×10^{-39} g cm^2 (1-D); $I^{\ddagger}/I = 4.28$
internal (active)	5×10^{-41} g cm^2 (1-D); $(\alpha_1)(6.25 \times 10^{-78})$ g^2 cm^4 (2-D)

$H_2O_4^{\ddagger}$ (Disproportionation Complex)

vibrations, cm^{-1}
3600 (2), 1300 (2), 800 (2), 700, 500 (3)
rotational moments of inertia, g cm^2
external (inactive) 6×10^{-39} (1-D); 13×10^{-39} (2-D)
internal (active) I_1 (1-D)

Best-Fit Parameters[b]

T, K	λ	α_1	$10^{43}I_1$, g cm^2	log $A_{1\infty}$	log $A_{2\infty}$	$10^{11}k_\infty$, cm^3 molecule^{-1} s^{-1}
241	0.48	0.27	3.7	16.9	11.3	11
269	0.42	0.20	3.0	16.6	11.1	6.6
298	0.40	0.17	2.5	16.3	11.0	4.8
344	0.37	0.14	2.5	16.0	10.9	3.6
417	0.33	0.10	3.1	15.4	10.9	2.0

[a] Parameters taken from ref 16. See text. [b] Obtained by using $E_1 = 20.0$ kcal mol^{-1}, $E_2 = 8.0$ kcal mol^{-1} (model II).

expects for a high-pressure limiting rate constant. However, the experimental data are so far away from the high-pressure limit that this result may be an artifact of the fitting procedure.

Deuterium Isotope Effect. The data in Table VI show that the A factors for the bimolecular and termolecular components of the $DO_2 + DO_2$ reaction are factors of 10 and 5 smaller, respectively, than the corresponding HO_2 values. The temperature dependence for the DO_2 bimolecular component, $E/R = -905$ K, is also substantially greater than for the HO_2 reaction, $E/R = -625$ K. Since $k_{2,H} \sim k_{2,D}$, it can be shown from the equations derived in the previous section that

$$\frac{k_{a2,H}}{k_{a2,D}} \approx \frac{k_{II,H}k_{III,D}}{k_{II,D}k_{III,H}}$$

This ratio was evaluated from the data in Tables II and IV and shows no discernible trend with temperature, within experimental scatter. An average value of 1.8 ± 0.7 was found for $k_{a2,H}/k_{a2,D}$ over the temperature range 240–417 K. The indication, therefore, is that at least half of the isotope effect arises from the tightening of the complex leading to the disproportionation channel upon deuteration. The remaining contribution may arise in the association reaction, which could be verified experimentally by examining the isotope effect on k_∞. Alternatively, the effect could be due to zero-point energy differences. If so, estimating the magnitude of the effect would be difficult due to the highly uncertain structures of the transition states.

Implications for Atmospheric Modeling. Combining all the pressure, temperature, and water vapor effects measured in this study, the overall value of k_1 is given by

$$k_1 = (2.2 \times 10^{-13} \exp(620/T) + 1.9 \times 10^{-33}[M] \exp(980/T))(1 + 1.4 \times 10^{-21}[H_2O] \exp(2200/T)) \text{ cm}^3 \text{ molecule}^{-1} \text{ s}^{-1}$$

This expression will be suitable for M = air over the temperature, pressure, and humidity conditions found in the atmosphere from ground level through the mesosphere. This expression may be compared with the one recommended in a recent (NASA) rate constant evaluation for stratospheric chemistry.[35]

$$k_1 = (3.4 + 3.4 \times 10^{-22}[M]T) \times 10^{-14} \exp(1150/T) \text{ cm}^3 \text{ molecule}^{-1} \text{ s}^{-1}$$

which uses the two-component pressure mechanism but has a much larger temperature dependence. Also, water vapor effects were not considered because of their negligible importance in the stratosphere. The altitude profiles of these two expressions are compared in Figure 8 by using a water vapor profile characteristic of the midlatitudes. Our expression yields significantly larger values below 6 km due primarily to the water vapor effect. The smaller temperature dependence, however, results in lower values of k_1 above this altitude. As indicated in the figure, the agreement between the two expressions in the troposphere is improved if our water vapor correction is used in the NASA expression. A temperature-dependent water vapor effect is clearly necessary for the accurate modeling of tropospheric H_2O_2 chemistry.

Reaction 1 is the only known homogeneous gas-phase source of H_2O_2 in the atmosphere. While the primary H_2O_2 removal process is photolysis, this species participates in a reaction cycle which destroys odd-hydrogen (HO_x) radicals:

$$HO_2 + HO_2 \rightarrow H_2O_2 + O_2$$

$$OH + H_2O_2 \rightarrow H_2O + HO_2$$

net: $$OH + HO_2 \rightarrow H_2O + O_2$$

This cycle is particularly important in the troposphere where it augments the direct reaction

$$OH + HO_2 \rightarrow H_2O + O_2$$

(35) W. B. DeMore, R. T. Watson, D. M. Golden, R. F. Hampson, M. Kurylo, C. J. Howard, M. J. Molina, and A. R. Ravishankara, JPL Publication 82-57, Jet Propulsion Laboratory, Pasadena, CA, 1982.

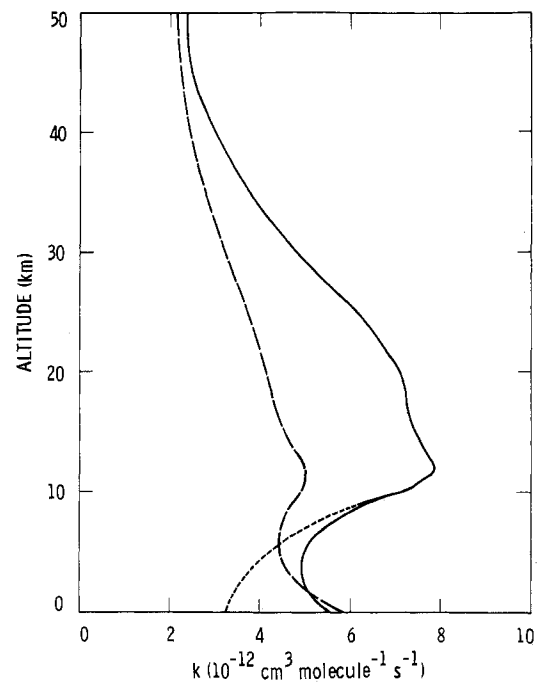

Figure 8. Rate constants for the $HO_2 + HO_2$ reaction vs. altitude for typical atmospheric conditions (average midlatitude water vapor profile): (—) rate constant expression from NASA review (ref 35) with water vapor correction from this work; (- - -) same as above without water vapor correction; (– – –) this work.

Since H_2O_2 lifetimes are reasonably short ($\sim$1 day) hydrogen peroxide will be in photochemical equilibrium and its concentration will be directly proportional to k_1. Accurate values of this rate constant are therefore required to predict the rate of HO_x removal in the troposphere and for comparison with ambient H_2O_2 concentration measurements.

Conclusions

Kinetics studies of the $HO_2 + HO_2$ and $DO_2 + DO_2$ reactions over the temperature range 240–417 K show that the reaction has both a zero-pressure bimolecular component and a termolecular component linearly dependent on pressure up to 700 torr. This behavior is indicative of a two-channel mechanism in which the H_2O_4 intermediate can disproportionate, dissociate back to reactants, or undergo collisional deactivation on comparable time scales. While the exact temperature dependence of k_1 is a function of total pressure, below 1 atm E/R is about (650 ± 50) K in agreement with the recent studies of Thrush and Tyndall,[7] Patrick and Pilling,[6] and Cox and Burrows[2] below 10 torr. The effect of added water vapor on the reaction rate is observed to be a strong function of temperature. However, the ratio $k_1/k_1([H_2O] = 0)$ is independent of the total pressure between 270 and 298 K which indicates that the mechanism proposed by Lii et al.[10] to account for the water vapor enhancement must be modified to include the details of the H_2O_4 unimolecular decomposition. The water vapor effect has a significant impact on hydrogen peroxide production in the troposphere and should be included in tropospheric chemical models.

The temperature and pressure dependence of the $HO_2 + HO_2$ reaction can be simulated with a two-channel RRKM model. A priori estimates of the vibrational frequencies of H_2O_4 based on the previous work of Tsang[16] lead to H_2O_4 binding energies which are unrealistically high (32 kcal/mol^{-1} for the initial association). In contrast, the weak binding predicted by the thermochemical estimates of Benson[25,26] ($\sim$6–9 kcal mol^{-1}) requires the use of an extremely loose model for H_2O_4. The best estimates of the binding energy for the assumed H_2O_4 intermediate in the open-chain configuration lie in the range 12–20 kcal mol^{-1} relative to HO_2; however, because many of the H_2O_4 structural properties are so poorly known, these estimates are highly uncertain.

Acknowledgment. The research described in this paper was carried out by the Jet Propulsion Laboratory, California Institute of Technology, under contract with the National Aeronautics and Space Administration. Many helpful discussions with J. J. Margitan, W. B. DeMore, J. H. Goble, M. J. Molina, L. Froidevaux, and R. A. Marcus are gratefully acknowledged. We also thank R. Patrick (SRI) for his useful comments on this manuscript.

Registry No. HO_2, 3170-83-0; DO_2, 13587-55-8.

Reactivity of OH with Tyrosine in Aqueous Solution Studied by Pulse Radiolysis

S. Solar, W. Solar, and N. Getoff*

Institut für Theoretische Chemie und Strahlenchemie der Universität Wien and Ludwig Boltzmann Institut für Strahlenchemie, A-1090 Wien, Austria *(Received: June 20, 1983)*

The specific OH attack on various sites of the tyrosine molecule in neutral aqueous solutions (pH 6–8), saturated with N_2O, has been investigated. The main process (~50%) is the formation of ortho-directed OH adduct (R_1) with $k = (7.0 \pm 0.5) \times 10^9$ dm^3 mol^{-1} s^{-1} (λ_{max} = 330 nm, $\epsilon_{330} = 300 \pm 30$ m^2 mol^{-1}), which decays by water elimination according to a first-order reaction ($k' = (1.8 \pm 0.2) \times 10^4$ s^{-1}) under formation of phenoxyl radical, as well as by second order with $2k = (3.0 \pm 1.0) \times 10^8$ dm^3 mol^{-1} s^{-1}. The phenoxyl radical is additionally formed as a primary product (~5%) with $k = (6.0 \pm 1.0) \times 10^8$ dm^3 mol^{-1} s^{-1}. It possesses two absorption maxima, 260 nm ($\epsilon_{260} = 600 \pm 50$ m^2 mol^{-1}) and 405 nm ($\epsilon_{405} = 260 \pm 20$ m^2 mol^{-1}), and decays with $2k = (4.0 \pm 1.0) \times 10^8$ dm^3 mol^{-1} s^{-1}). The meta isomer of the OH adducts (R_2) is formed to ~35% with $k = (5.0 \pm 0.4) \times 10^9$ dm^3 mol^{-1} s^{-1}, having two absorption maxima at 305 nm ($\epsilon_{305} = 280 \pm 30$ m^2 mol^{-1}) and 540 nm ($\epsilon_{540} = 23 \pm 3$ m^2 mol^{-1}), and disappears with $2k = (2.0 \pm 0.5) \times 10^9$ dm^3 mol^{-1} s^{-1}. The rest of ~10% OH radicals attack most probably the para and to a small extent ipso positions of the phenol ring under formation of the corresponding adducts. The H abstraction from the alanine moiety cannot be excluded.

Introduction

The aromatic amino acids represent an essential part of proteins and hormones, and the elucidation of their reaction mechanism with the primary water radiolytic products, particularly the OH attack on these molecules, is of special importance for radiobiology and radiation chemistry. Pulse radiolysis of tyrosine and phenylalanine has been already carried out at different pH's.[1] In the case of tyrosine a simultaneous formation of OH-addition transients (absorption bands at 310 and 320 nm) and phenoxyl radicals (λ_{max} = 405 nm) has been observed. In neutral media the latter results from a direct OH reaction with the hydroxyl group of the substrate as well as from water elimination from the corresponding cyclohexadienyl radicals. The total rate constant (k_t) for OH attack on tyrosine at pH 4 has been determined to be k_t(OH + tyrosine) = 4.2×10^9 dm^3 mol^{-1} s^{-1},[1] and $k = 1.4 \times 10^{10}$ dm^3 mol^{-1} s^{-1}.[2] For the uncatalyzed water elimination (pH ~7) a first-order rate constant of $k = 1 \times 10^3$ s^{-1} has been established.[3] The attack of various radical anions such as $SO_4^{-}\cdot$, $Br_2^{-}\cdot$, etc.[4,5] and $N_3\cdot$[6] on tyrosine, leading to formation of phenoxyl radical, has been also reported.

An attempt has now been made to obtain more information about the specific OH reaction on various sites of the tyrosine molecule in neutral aqueous solution. The investigations were focused on the resolution of the distinct absorptions of the transients, obtained by pulse radiolysis, and on determining their individual kinetic and spectroscopic parameters. A semilinear optimization procedure[7,8] subsequent to the registration of the transient absorption change as a function of time was used to master this problem.

Experimental Section

The chemicals were of purest grades available (E. Merck, Darmstadt, F.R.G.). The solutions of tyrosine (5×10^{-6}–10^{-4} mol dm^{-3}) were prepared using four times freshly distilled water, and the pH 6–8 was adjusted by means of aqueous barium hydroxide. In order to convert e_{aq}^- into OH, the solutions were saturated with N_2O ($k(e_{aq}^- + N_2O) = 9.1 \times 10^9$ dm^3 mol^{-1} s^{-1})[9] and irradiated in a suprasil quartz cell (3 × 2 cm light path) with 400-ns pulses from a 3-MeV Van de Graaff accelerator (Type K, High Voltage Ing. Corp., Burlington, VT). The applied dose per pulse was ~5 J kg^{-1} (~0.5 krd). An XBO 450-W Xenon lamp (Osram) served as the analyzing light source. A double-prism monochromator (Zeiss MM12) combined with a wide-range sensitivity photomultiplier (Hamamatsu, R 955) rendered the kinetic and spectroscopic measurements. The data were digitized with a Biomation 8100 transient recorder and processed by a minicomputer (PDP-11/10, DEC) for averaging a large number of measurements. The final mean value of the stored traces was transferred to another computer (PDP-10, DEC), where the data collection program was run. Finally, each trace was displayed in 100 points, normalized for dose, and averaged for improving the signal to noise ratio. Details on the pulse radiolysis equipment and dosimetry have been previously reported.[10,11]

Computation Method

Based on the measurements of the time-dependent change of the optical densities of the irradiated solutions (time range 1–2000 μs, using three different solute concentrations), the applied computation method permits one to resolve individually the kinetic and spectroscopic parameters in such a way that the observed course of the chemical processes is reproduced by the proposed reaction model in an optimal way. The Gear integration routine[12–14] was used, including some essential modifications for

(1) J. Chrysochoos, *Radiat. Res.*, **33**, 465 (1968).
(2) J. Feitelson and E. Hayon, *J. Phys. Chem.*, **77**, 10 (1973).
(3) E. J. Land and M. Ebert, *Trans. Faraday Soc.*, 1181 (1967).
(4) M. L. Posener, G. E. Adams, P. Wardman, and R. B. Cundall, *J. Chem. Soc., Faraday Trans. 1*, **72**, 2231 (1976).
(5) K. M. Bansal and R. W. Fessenden, *Radiat. Res.*, **67**, 1 (1976).
(6) A. Singh, G. W. Koroll, and R. B. Cundall, *Radiat. Phys. Chem.*, **19**, 137 (1982).
(7) S. Solar, W. Solar, and N. Getoff, *J. Chem. Soc., Faraday Trans. 2*, **79**, 123 (1983).
(8) S. Solar, W. Solar, and N. Getoff, *Radiat. Phys. Chem.*, **21**, 129 (1983).
(9) E. Janata and R. H. Schuler, *J. Phys. Chem.*, **86**, 2078 (1982).
(10) N. Getoff and F. Schwörer, *Radiat. Res.*, **41**, 1 (1970).
(11) N. Getoff and F. Schwörer, *Int. J. Radiat. Phys. Chem.*, **5**, 101 (1973).
(12) C. W. Gear in "Numerical Initial Value Problems in Ordinary Differential Equations", Prentice-Hall, Englewood Cliffs, NJ, 1971, Chapter 11.
(13) C. W. Gear, *Commun. ACM*, **14**, 176 (1971).

0022-3654/84/2088-2091$01.50/0